Acta Crystallographica Section B
Structural Science
ISSN 0108-7681

Hydrogen-bridged chelate ring-assisted π-stacking interactions

Hasan Karabıyık,[a]* Hande Karabıyık[a] and Nazan Ocak İskeleli[b]

[a]Department of Physics, Dokuz Eylül University, Buca, İzmir 35160, Turkey, and [b]Science Education Department, Ondokuz Mayıs University, Kurupelit, Samsun 55139, Turkey

Correspondence e-mail: hasan.karabiyik@deu.edu.tr

Received 25 July 2011
Accepted 6 December 2011

A salicylideneaniline (SA) derivative, (6*Z*)-6-({[2-(hydroxymethyl)phenyl]amino}methylidene)-3,5-dimethoxycyclohexa-2,4-dien-1-one monohydrate, has an increased aromaticity within its hydrogen-bridged chelate ring owing to its NH character. In the reported crystal structure, nonconventional π-stacking interactions, which are referred to as *hybrid* π-stacking interactions, are observed between a quasiaromatic chelate ring, formed as a result of the resonance-assisted intramolecular hydrogen bond and ordinary aromatic rings. Besides, π-stacking interactions are also seen between two hydrogen-bridged quasiaromatic chelate rings, which are referred to as *pure* π-stacking interactions. A CSD search has revealed that both kinds of interactions are frequently observed in molecular crystals of SA derivatives in fully or partially NH tautomeric form, and aromaticity levels of certain fragments of SA derivatives have dramatic effects on their stacking arrangements. These interactions are distinguished from the usual $\pi\cdots\pi$ interactions by their formation character, *i.e.* both σ- and π-deficient and σ-deficient character of pure interactions is more pronounced than that of the hybrid ones.

1. Introduction

The importance of stacking interactions involving aromatic π-systems has been shown for various types of molecular crystals (Kar *et al.*, 2008; Churchill & Wetmore, 2009; Reger *et al.*, 2009; Schneider, 2009; Holy *et al.*, 2009; Ringer & Sherrill, 2009; Zheng *et al.*, 2010; Egbe *et al.*, 2010). Intermolecular interactions relating to aromatic moieties such as $\pi\cdots\pi$ stacking are important in supramolecular chemistry, materials science and even biochemistry (Tsuzuki, 2005). It is well known that π–π interactions are very difficult to control owing to their lack of strength and directionality (Noveron *et al.*, 2002; Garcia-Baez *et al.*, 2003; Olenik *et al.*, 2003; Marsden *et al.*, 2005). However, there are some literature examples describing the influence of π–π interactions on the formation of special molecular arrangements (Yang *et al.*, 2009; Blanco *et al.*, 2009; Kumagai *et al.*, 2009; Banerjee *et al.*, 2009; Reger *et al.*, 2010). Planar chelate rings in transition metal complexes called metallacycles can also participate in stacking interactions similar to those of aromatic organic molecules (Bogdanovic *et al.*, 2002; Castiñeiras *et al.*, 2002; Tomic *et al.*, 2003; Craven *et al.*, 2003; Mukhopadhyay *et al.*, 2004; Tomic *et al.*, 2004; Medaković *et al.*, 2004; Philip *et al.*, 2004; Tsubaki *et al.*, 2005; Tomic *et al.*, 2006; Allali *et al.*, 2009) and are of importance in terms of crystal engineering and design considerations (Sredojevic *et al.*, 2010). The presence of such interactions is regarded as structural evidence for metalloaromaticity (Masui, 2001; Fernandez *et al.*, 2009; Karabiyik *et al.*, 2010).

At this point, the question whether chelate rings not mediated by a metal ion, namely hydrogen-bridged quasi-rings in organic compounds, can participate in π-stacking interactions is still an intriguing item for crystal engineering and sustains its timeliness. In principle, there is no impediment for the observation of such π-stacking interactions, but there have not been any articles published yet on this topic. Aromatic Schiff bases are one of the most promising chemical species to be considered for this purpose because of their structural and electronic properties mentioned below. The structures of *ortho*-hydroxy aromatic Schiff bases, in particular salicylideneaniline (SA) derivatives, have received much attention owing to their keto–phenol (or NH OH) tautomerism (Fabian *et al.*, 2004; Amimoto & Kawato, 2005; Filarowski, 2005; Filarowski *et al.*, 2005; Petek *et al.*, 2008, 2010; Karabiyik *et al.*, 2009, 2011). Depending on the position of the tautomeric proton, two types of intramolecular hydrogen bonds are possible, O—H···N and O···H—N, in phenol (OH) and in *cis*-keto (NH) tautomers, respectively. Although Schiff bases exhibit two well known tautomeric forms, OH and NH, another structural form referred to as the zwitterion is also possible. The zwitterionic form is regarded as a variant of the NH form, but the two forms can be easily distinguished from canonic *cis*-keto tautomers with the aid of their N^+—H bond distances (Karabiyik *et al.*, 2008). Zwitterionic forms of Schiff bases have a resonance-assisted ionic intramolecular hydrogen bond (N^+—H···O^-; Krygowski *et al.*, 1997; Dominiak *et al.*, 2003; Petek *et al.*, 2006; Karabıyık *et al.*, 2007, 2008), and their N^+—H bonds are considerably longer than the standard interatomic separations observed in neutral N—H bonds (Steiner, 1998). Heteronuclear intramolecular hydrogen bonds in SA derivatives are the most important phenomenon due to its resonance-assisted nature, affecting the electronic states of its neighboring aromatic fragments (Dziembowska & Rozwadowski, 2001; Grabowski, 2001, 2002, 2003, 2007; Filarowski *et al.*, 2002; Sobczyk *et al.*, 2005; Palusiak & Krygowski, 2007). The NH form of SA derivatives in crystals can be regarded as a resonance hybrid of two canonical structures: the *cis*-keto tautomer and zwitterionic form, having identical atomic positions but a different covalent skeleton (Filarowski, 2005; Filarowski *et al.*, 2005; Karabiyik *et al.*, 2009, 2011; Petek *et al.*, 2010) as shown in Fig. 1.

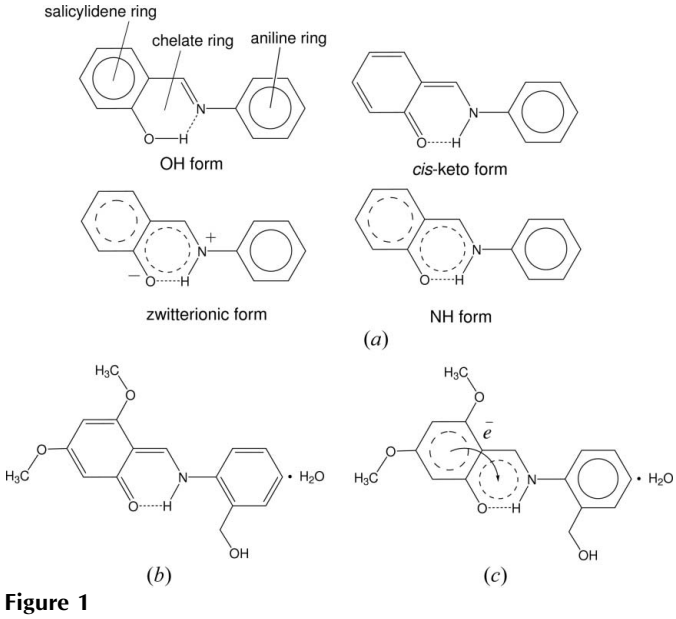

Figure 1
(*a*) Possible tautomeric forms of SA, (*b*) chemical diagram of the compound studied, (6*Z*)-6-({[2-(hydroxymethyl)phenyl]amino}methylidene)-3,5-dimethoxycyclohexa-2,4-dien-1-one monohydrate, and (*c*) chart showing aromaticity situations of the rings together with the electron transfer route in the compound studied. The *cis* labeling is based on the relative positions of the tautomeric H and O atoms in an *ortho* position. Partial aromatic rings are represented by dashed circles. Dash widths are illustrated to be inversely proportional to the associated ring aromaticity.

Analysis of the effects of tautomerism of SA derivatives has revealed the importance of the concept of aromaticity balance (Filarowski, 2005; Filarowski *et al.*, 2005; Karabiyik *et al.*, 2009, 2011; Petek *et al.*, 2010). Aromaticity balance means that there is a π-electron donation from the salicylidene to the chelate ring, revealing itself by a decrease in aromaticity of the former and an increase in aromaticity of the latter. The augmented aromaticity within the chelate ring is closely related to the predominancy of the NH character of a SA derivative (Karabiyik *et al.*, 2009; Petek *et al.*, 2010; Karabiyik *et al.*, 2011). This structural aspect regarding aromatic Schiff bases may deeply influence our understanding of $\pi\cdots\pi$ stacking interactions and offers an opportunity to diversify the types of rings participating in π-stacking interactions.

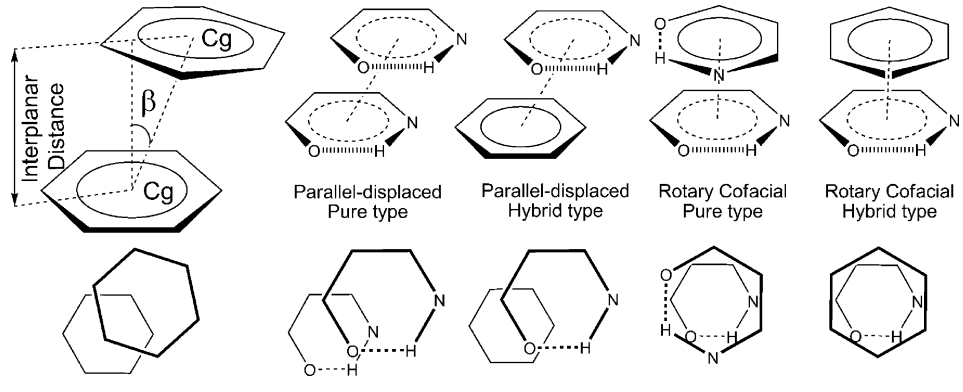

Figure 2
General definition of a conventional $\pi\cdots\pi$ interaction geometry and schematic view of *pure* and *hybrid* hydrogen-bridged ring-assisted π-stacking interactions. The lower band shows their views from above.

In this study we present the molecular and crystal structure of one of the SA derivatives, in particular its unusual π-stacking interactions. To the best of our knowledge, this is the first study on hydrogen-bridged rings participating in $\pi\cdots\pi$ stacking interactions. Since such π-stacking

Table 1
Experimental details.

Crystal data	
Chemical formula	$C_{16}H_{17}NO_4{\cdot}H_2O$
M_r	305.32
Crystal system, space group	Triclinic, $P\overline{1}$
Temperature (K)	296
a, b, c (Å)	5.0816 (6), 11.0087 (12), 14.5301 (16)
α, β, γ (°)	108.935 (8), 97.042 (9), 93.092 (9)
V (Å^3)	759.24 (15)
Z	2
Radiation type	Mo $K\alpha$
μ (mm^{-1})	0.10
Crystal size (mm)	0.65 × 0.31 × 0.06
Data collection	
Diffractometer	Stoe IPDS-2
Absorption correction	–
No. of measured, independent and observed [$I > 2\sigma(I)$] reflections	12 593, 2989, 1913
R_{int}	0.050
Refinement	
$R[F^2 > 2\sigma(F^2)]$, $wR(F^2)$, S	0.057, 0.158, 0.97
No. of reflections	2989
No. of parameters	275
No. of restraints	3
H-atom treatment	H-atom parameters fully refined
$\Delta\rho_{max}$, $\Delta\rho_{min}$ (e Å^{-3})	0.16, −0.16

Computer programs used: *X-AREA* (Stoe & Cie, 2002*a*), *X-RED* (Stoe & Cie, 2002*b*), *SHELXS*97 (Sheldrick, 2008), *SHELXL*97 (Sheldrick, 2008). For further information regarding the restraints applied in crystal structure refinement, see §2.2.

interactions are closely related to the π-delocalization level of certain molecular fragments, our scientific attention is inevitably directed towards details of the molecular structure. At this point, the aromaticities of π-electron-donating salicylidene and the π-electron-accepting chelate ring play an essential role in the understanding and assessment of these new types of $\pi\cdots\pi$ stacking interactions. These novel interactions are split into two subclasses: pure and hybrid $\pi\cdots\pi$ stacking interactions. As shown in Fig. 2, the statement '*pure*' emphasizes that both rings participating in the interactions have the same formation character (hydrogen-bridged), while the statement '*hybrid*' qualifies the difference between the formation characters of the rings participating in such interactions, *i.e.* hydrogen-bridged and conventional six-membered.

Aromatic rings can interact in different relative orientations, for example, face-to-face (cofacial), offset (parallel-displaced) and point-to-face (T-shaped; Janiak, 2000; Hunter *et al.*, 2001; Lee *et al.*, 2005; Wu *et al.*, 2009), and have been found to be a useful tool in the manipulation of the molecular building blocks in crystals (Dance, 2003; Serrano-Becerra *et al.*, 2009). Since the hydrogen-bridged quasiaromatic chelate ring in SA derivatives is fused with the substituted salicylidene ring, these fragments tend to orient their planes in parallel in the crystal phase. Therefore, our particular interest has been focused on the offset (or parallel-displaced) and rotary cofacial stacking interactions as shown in Fig. 2. Such interactions are of great importance in crystal engineering owing to the fact that changes in molecular geometries of SA derivatives are accompanied by noncovalent interactions in their molecular crystals and *vice versa*. Molecules of thermochromic SA derivatives in the NH form are essentially planar in the solid state and stacked in a parallel fashion with a short spacing below 4 Å, while photochromic ones are distinctly non-planar and loosely packed and these phenomena are topochemically dominated (Cohen & Schmidt, 1962; Cohen *et al.*, 1964).

2. Experimental and methodology

2.1. Preparation and characterization of the compound

The compound (6*Z*)-6-({[2-(hydroxymethyl)phenyl]amino}-methylidene)-3,5-dimethoxycyclohexa-2,4-dien-1-one monohydrate (the lowest part in Fig. 1) was prepared by refluxing a mixture of a solution containing 2-hydroxy-4,6-dimethoxybenzaldehyde (0.0205 g 0.11 mmol) in 20 ml of ethanol and a solution containing (2-aminophenyl)methanol (0.0139 g 0.11 mmol) in 20 ml of ethanol. The reaction mixture was stirred for 1 h under reflux. The crystals of 2-[(2-methanol-phenylimino)methyl]-3,5-dimethoxyphenol suitable for X-ray analysis were obtained from ethylalcohol by slow evaporation (yield: 74%; m.p. 408–410 K). Anal.: calc. for $C_{16}H_{17}NO_4{\cdot}H_2O$: C 62.94, H 6.27, O 26.20, N 4.59; found: C 62.96, H 6.28, O 26.24, N 4.52. ^{1}H NMR ($CDCl_3$ δ in p.p.m. from TMS): 3.84 (s, 6H, O—CH_3), 4.66 (s, 2H, —CH_2—), 5.47 (s, 1H, —CH$_2$—O*H*), 6.85–8.24 (m, 6H, Ar—*H*), 8.97 (d, 1H, C*H* = NH, $^3J_{CH-NH}$ = 7.5 Hz), 14.46 (d, 1H, CH = N*H*, $^3J_{NH-CH}$ = 7.5 Hz). ^{13}C NMR (δ in p.p.m., $CDCl_3$): 55.78 (two overlapped peaks, O—*C*H$_3$), 60.62 (Ar—*C*H$_2$—OH), 85.83, 88.4, 110.38, 124.48 (two overlapped peaks, Ar *C*), 126.32, 128.68, 140.74, 141.58, 146.78 (*C*—N), 162.88, 176.37, 182.38 (*C*═O). FT–IR (KBr, ν, cm^{-1}): 3300–3550 (*br*, O—H), 3242 (Ar CH stretching), 1626 (C═O), 1337 (C—N stretching). The IR spectra of the compound unambiguously show the presence of water, with several peaks at 3300–3550 cm^{-1} overlapping the *broad* OH absorption band and a smooth shoulder near 1620 cm^{-1} corresponding to the stretching and bending modes. UV–vis spectra (nm) in solution (EtOH): 297 (log ε = 0.349), 331 (log ε = 0.370), 389 (log ε = 0.389).

2.2. X-ray crystallography and treatment of H atoms

X-ray measurements were made on a Stoe IPDS 2 diffractometer. Cell parameters were determined using *X-AREA* (Stoe & Cie, 2002*a*) software. All data were corrected for Lorentz and polarization effects by *X-RED*32 software (Stoe & Cie, 2002*b*). The structure was solved by direct methods *via* the *WinGX* (Farrugia, 1999) program suit and refined on F^2 by a full-matrix least-squares procedure using anisotropic displacement parameters for all non-H atoms (Sheldrick, 2008). All H atoms in the compound were located by a difference-Fourier method, and their positional and isotropic displacement parameters were fully refined. In the final refinement cycle, the *SHELXL*97 (Sheldrick, 2008) instruction SADI was used to restrain the O—H distances of the water moiety so as to be similar to each other, within an effective standard uncertainty of 0.03. The positions of the water H atoms were refined subject to a H···H DANG

Table 2
Selected geometric parameters (Å, °) of the compound.

N1—C7	1.312 (3)	C6—C5	1.433 (3)
N1—C13	1.414 (3)	C5—C4	1.355 (4)
O5—C5	1.361 (3)	C4—C3	1.411 (4)
O3—C3	1.360 (3)	C3—C2	1.357 (3)
O1—C1	1.279 (3)	C2—C1	1.422 (3)
C6—C7	1.386 (3)	O2—C14	1.423 (3)
O1—C1—C2	121.4 (2)	N1—C7—C6	123.8 (2)
O1—C1—C6	120.6 (2)	N1—C13—C12	117.5 (2)
C3—C2—C1—O1	−178.3 (3)	C1—C6—C7—N1	1.5 (4)
C7—C6—C1—O1	−1.6 (4)	C5—C6—C7—N1	−178.6 (3)

Table 3
Geometric details (Å, °) of intra- and intermolecular hydrogen bonds of the compound.

D—H···*A*	*D*—H	H···*A*	*D*···*A*	∠*D*—H···*A*
N1—H1···O1	0.84 (3)	1.88 (3)	2.587 (3)	142 (2)
O5*W*—H6*W*···O2	0.81 (3)	2.10 (3)	2.915 (3)	178 (4)
O2—H21···O1^{i}	0.89 (3)	1.82 (4)	2.710 (2)	174 (3)
C51—H51*B*···O3^{ii}	1.05 (4)	2.63 (4)	3.048 (4)	103 (2)
O5*W*—H5*W*···O5*W*^{iii}	0.80 (3)	2.32 (3)	2.819 (6)	121 (3)

Symmetry codes: (i) $-x+1, -y+1, -z+1$; (ii) $-x-1, -y+1, -z$; (iii) $-x+1, -y, -z+1$.

restraint of 1.40 Å with an e.s.d. value of 0.04. In order to generate acceptable hydrogen bonds of the solvent water molecule which are consistent with the diffraction data, a BUMP restraint (Müller *et al.*, 2006) was used with a standard uncertainty of 0.06. Details of crystal data, data collection and refinement are shown in Table 1.[1]

2.3. Assessment of aromaticities

Since aromaticity is not an observable and, therefore, not a directly measurable quantity, there are many different experimental and theoretical methodologies in order to describe the quantitative expression of aromaticity thorough analysis of various structural, magnetic, thermodynamic and kinetic factors (Schleyer *et al.*, 1996; Schaad & Hess, 2001; Cyrañski *et al.*, 2002; Cyrański *et al.*, 2003; Krygowski & Cyrański, 2004; Cyrański, 2005; Chen *et al.*, 2005; Ośmiałowski *et al.*, 2006). Geometry-based structural definitions of aromaticity by means of numerical indicators known as indices of aromaticity have received much attention in recent years (Bultinck *et al.*, 2006). Among geometry-based measures of π-electron delocalization, the harmonic oscillator model of aromaticity (HOMA) index (Krygowski, 1993) is one of the most widespread and effective indices used for describing aromaticity based on structural criteria (Krygowski & Cyrański, 2001). It is commonly accepted that aromaticity indices based purely on the electron density function, such as the Para Delocalization Index (PDI) or FLU index, are more reliable than others (Poater *et al.*, 2005), since they directly reflect electron delocalization, underlying the concept of aromaticity. However, their computational cost is higher than most of the other aromaticity indices due to the fact that these computations require the determination of atomic basins by topological analyses on electronic density and subsequent computation of the MO overlap integrals, which are necessary to calculate multicenter delocalization indices. On the other hand, magnetic indices used to describe aromaticity such as NICS (Nucleus-Independent Chemical Shift) have some imperfections for chemical species having π-stacked aromatic rings due to the coupling between the magnetic fields generated by the two stacked moieties (Osuna *et al.*, 2006). In spite of these, the HOMA index is easily accessible and correlates well with aromaticity indices based purely on an electron density function such as PDI (Poater *et al.*, 2003, 2005). The HOMA index is equal to 1 for fully aromatic systems and 0 for nonaromatic systems. The HOMA indices describe the average squared deviation of bond lengths from their optimal value as

$$\mathrm{HOMA} = 1 - \frac{1}{n}\sum_{j=1}^{n} \alpha_j \left(R_j - R_{\mathrm{opt}}\right)^2 \qquad (1)$$

where n is the number of bonds, R_j stands for the individual bond length, α_j is a normalization constant which is equal to 257.7 for C—C, 93.52 for C—N and 157.38 for C—O bonds, fixed to give HOMA = 0 for nonaromatic Kekulé systems and HOMA = 1 for purely aromatic systems with all bonds equal to the optimal value R_{opt} = 1.388 Å for C—C, R_{opt} = 1.334 Å for C—N, R_{opt} = 1.265 Å for C—O (Krygowski, 1993).

3. Results and discussion

3.1. Molecular structure of the compound

The molecular geometry of the compound is shown in Fig. 3 and its selected geometric parameters are given in Table 2. The dihedral angle between two aromatic rings defined by atoms C1–C6 and C8–C13 is 2.2 (2)°, indicating the near coplanarity of two rings. Keeping in mind that the molecular geometries of SA derivatives in NH tautomeric form are essentially planar (Karabiyik *et al.*, 2009, 2011), this result is as expected. The dihedral angle between the substituted salicylidene and chelate ring is only 1.3 (5)°, because of active electronic charge transfer through π-delocalized systems of two fused fragments. A strong intramolecular hydrogen bond of the type N—H···O (Table 3) adds to the planarity of these adjacent moieties. The tautomeric proton (H1) deviates slightly from the mean chelate plane by −0.02 (1) Å and a slightly large value of the valence angle N1—C7—C6 (Table 2) allows chelate ring strain to be reduced from the intramolecular hydrogen bond.

The HOMA index is a useful structural probe used in detecting charge transfer between adjacent molecular fragments (Karabiyik *et al.*, 2010) and in collectively describing a degree of bond-length variation within the rings involving proton transfer (Karabiyik *et al.*, 2009; Petek *et al.*, 2010). Using the bond lengths listed in Table 2, the HOMA indices for the substituted salicylidene (through C1/C6) and chelate

[1] Supplementary data for this paper are available from the IUCr electronic archives (Reference: RY5040). Services for accessing these data are described at the back of the journal.

ring are found as 0.627 and 0.793, respectively. Owing to the π-electron donation from the substituted salicylidene to the chelate ring, the π-electron delocalization level of the substituted salicylidene ring is considerably decreased, while that of the chelate ring is remarkably increased. The important result is also that the aromaticity of the chelate ring is greater than that of the salicylidene ring.

3.2. Do hydrogen-bridged rings really participate in π-stacking interactions?

The NH tautomeric character of the compound implies augmented electron delocalization within the chelate ring (Karabiyik *et al.*, 2009, 2011; Petek *et al.*, 2010). The results in §3.1 suggest that the quasiaromatic chelate ring is established at the expense of the aromaticity of salicylidene as a result of charge transfer from the salicylidene to the chelate ring. This fact is the physical basis underlying the participation of chelate rings in $\pi\cdots\pi$ stacking interactions.

One might ask the question whether a ring with an aromaticity level in the range 0.63–0.79 can be involved in a $\pi\cdots\pi$ stacking interaction and whether the hydrogen-bridged rings allow a sufficient intermolecular overlap of *p*-orbitals in the π-conjugated molecular fragments, necessary for $\pi\cdots\pi$ stacking interactions? It has been previously reported that the salicylidene ring whose aromaticity level as measured by the HOMA index is only 0.663 can indeed participate in the usual $\pi\cdots\pi$ interaction (Karabiyik *et al.*, 2009) and that the low lying formally vacant *p*-type orbital on the tautomeric proton of SA mediates the electronic charge transfer through the π-delocalized systems of the adjacent fragments (Karabiyik *et al.*, 2009, 2011). Thus, it can be stated that a ring current through the NCCCOH pathway appears within the quasiaromatic chelate ring allowing sufficient intermolecular overlapping of the *p*-orbitals, and its strength increases with the increasing NH character of the tautomer. In addition, according to Hunter–Sanders rules (Hunter & Sanders, 1990; Hunter, 1993, 1994; Cozzi *et al.*, 1993) the order of stability in the interaction of two π systems increases with decreasing electronic charge of the interacting π-delocalized fragments. The π-deficient character of the stacking interactions involving hydrogen-bridged rings not only does not prevent the occurrence of such interactions but improves the stability of the two interacting π-systems.

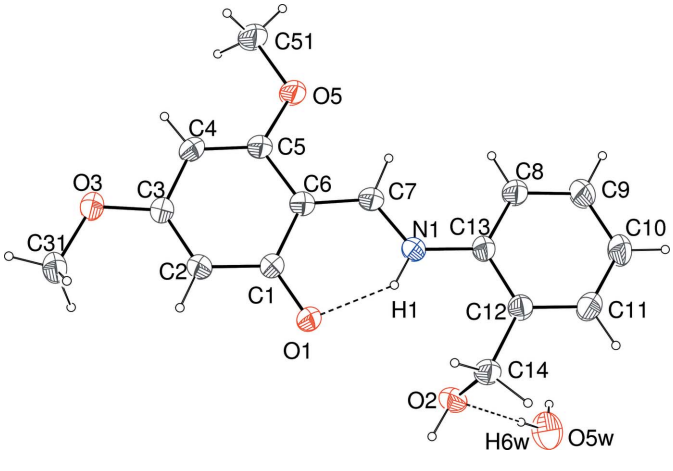

Figure 3
Displacement ellipsoid view and intramolecular hydrogen bonds of the investigated compound with atomic numbering scheme for non-H atoms. Displacement ellipsoids are drawn at the 30% probability level. Hydrogen bonds are displayed as dashed lines. *ORTEP*3 (Farrugia, 1997) representation: H atoms are shown as small spheres of arbitrary radii.

3.3. Intermolecular interactions and the role of hydrogen-bridged π-stacking interactions

The crystal structure reveals the formation of two supramolecular synthons $R_2^2(20)[2S(6)]$ and $R_2^2(14)$ (for graph notation see Bernstein *et al.*, 1995) as shown in Fig. 4. The synthons are built of O2—H21$\cdots$O1^{i} and C51—H51*B*$\cdots$O3^{ii} intermolecular hydrogen bonds. The geometric details for these bonds are given in Table 3. In addition, water molecules are involved in the formation of a diamond-shaped $R_2^2(4)$ synthon with the aid of the O5*W*—H5*W*$\cdots$O5*W*^{iii} intermolecular tandem hydrogen bond as shown in Fig. 5. When centrosymmetric $R_2^2(4)$ and $R_2^2(20)[2S(6)]$ synthons are interconnected by intermolecular O5*W*—H6*W*$\cdots$O2 hydrogen bonds, a chain is generated by translation along the *b* axis of the unit cell.

Interconnecting 6-((2-(hydroxymethyl)phenylamino)-methyl)-3,5-dimethoxycyclohexa-2,4-dienone molecules with $R_2^2(4)$ synthons of the water molecules, staircase-like chains are formed as shown in Fig. 5. Staircase-like chains are aligned back-to-back along the **a** direction of the unit cell. There are two noteworthy interatomic contacts, which contribute to the stabilization of this chain. The interatomic separation from O5*W* at (*x*, *y*, *z*) to O5*W* at $(2-x, -y, 1-z)$ is 2.860 (6) Å, which is smaller than the sum of their non-covalent radii (3.04 Å; Bondi, 1964). The almost planar molecular geometry of the compound means that both the salicylidene and aniline ring participate in such interactions. The relevant centroid names of hybrid $\pi\cdots\pi$ stacking interactions are Cg1 for the chelate, Cg2 for the substituted salicylidene (C1–C6) and Cg3 for the phenylmethanol ring (C8–C13). The centroid–centroid separation from Cg1 at (*x*, *y*, *z*) to Cg2 at [(iv) $x+1$, *y*, *z*] and from Cg1 at (*x*, *y*, *z*) to Cg3 at [(v) $x-1$, *y*, *z*] are 3.710 (7) and 3.678 (7) Å. Interplanar distances between the relevant

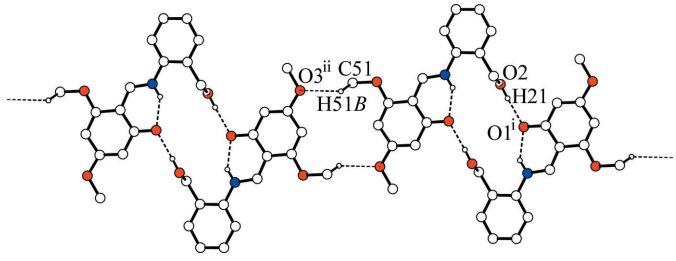

Figure 4
The formation of hydrogen-bonded supramolecular synthons of the compound viewed down the *b* direction.

centroids [Cg1···Cg2^{iv} = 3.373 (7) Å and Cg1···Cg3^{v} = 3.426 (7) Å] indicate the centroid slippage of 1.545 (7) Å for Cg1···Cg2^{iv} and of 1.338 (7) Å for Cg1···Cg3^{v}. It is inferred from these results that both $\pi\cdots\pi$ interactions are not exactly cofacial ($\beta \neq 0$, Fig. 2). The slippage angle β is 24.61 (5)° for Cg1···Cg2^{iv} and 21.33 (6)° for Cg1···Cg3^{v}.

For the description of distortions from an 'ideal' cofacial π-stack, the phenomenological approach of Curtis *et al.* (2004) has been applied. Examination of the values of the *pitch* and *roll* parameters [pitch (*P*) and roll (*R*) angles and pitch (*dp*) and roll (*dr*) distances] and of the extent of the overlap area of the adjacent π-stacked molecules (*AO*), calculated according to one of the models of Janzen *et al.* (2004), indicates that the solid-state packing provides a considerable spatial overlap between molecules in the π-stack (P_{12} = 47.12° > R_{12} = 21.80°, dp_{12} = 3.632 Å > dr_{12} = 1.349 Å, AO_{12} = 29.42% and P_{13} = 47.68° > R_{13} = 21.99°, dp_{13} = 3.762 Å > dr_{13} = 1.383 Å, AO_{13} = 29.11%, where the subscripts represent the relevant centroid numbers of the rings involved in the $\pi\cdots\pi$ interactions). Although both $\pi\cdots\pi$ interactions are not strictly cofacial, it can be stated that they allow substantial π-overlap between adjacent molecules, since the pitch distances (or angles) of both interactions are longer than their corresponding roll distances (or angles).

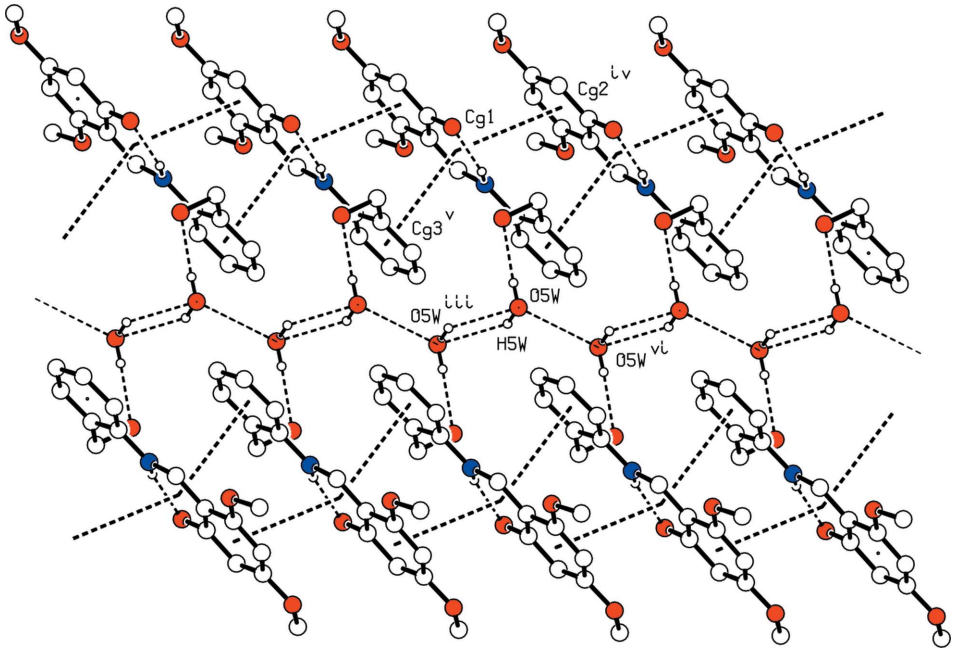

Figure 5
Viewed along the *a* direction water-directed aggregation of molecules stabilized by hybrid $\pi\cdots\pi$ interactions (*PLATON*, Spek, 2009). The centroids of the interacting ring pairs are connected by dashed lines. For the sake of clarity, H atoms not involved in this structural pattern have been omitted. Symmetry codes: (iii) $-x+1, -y, -z+1$; (iv) $x+1, y, z$; (v) $x-1, y, z$; (vi) $-x+2, -y, -z+1$.

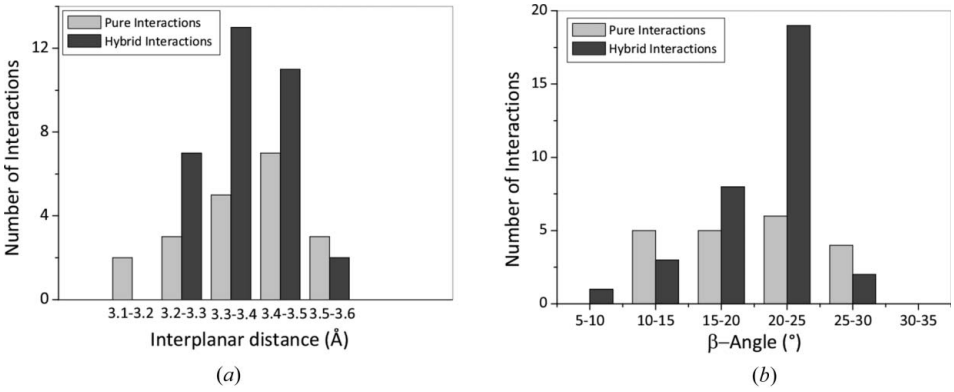

Figure 6
Histograms showing the distribution of the interplanar distances and of the slippage angles (β) for the interactions considered here.

4. CSD survey

To get an idea of the incidence of such π-stacking interactions and their efficiency, a Cambridge Structural Database (CSD) search was carried out with the help of the *ConQuest*1.3 program in the May 2010 release of the CSD, Version 5.31 (Bruno *et al.*, 2002). The program was used to retrieve structures satisfying the following criteria:

(i) the crystallographic *R* factor ≤ 10%;

(ii) error-free coordinates according to the criteria used in the CSD system;

(iii) including crystallographic disorder and ionic structures.

It was considered that an interaction existed if the dihedral angle between the mean planes of the two rings was less than 10° and the distance between the centres of the two rings was less than 3.8 Å. Probability-weighted coordinates for the tautomeric H atoms in disordered entities were used in determining the relevant centroids. A search on SA derivatives in purely and partly NH tautomeric form, including their zwitterionic forms, results in 49 hits. 43 of these show hydrogen-bridged ring-assisted π-stacking interactions. A total of 53 interactions were detected for 43 different SA derivatives, including those presented herein. This illustrates that such interactions are frequently observed in molecular crystals of SA derivatives in the NH tautomeric form.

Of these 53 interactions 10 are formed between hydrogen-bridged chelate and aniline rings (hybrid), 20 between two hydrogen-bridged chelate rings (pure) and 23 between hydrogen-bridged chelate and substituted salicylidene rings

(hybrid). The number of hybrid hydrogen-bridged ring-assisted π-stacking interactions exceeds that of pure ones. Furthermore, the fused aromatic fragments in SA derivatives, *i.e.* salicylidene and chelate rings, are much more frequently involved in hydrogen-bridged ring-assisted π-stacking interactions than are the aniline rings. These fragments are almost coplanar in all the chemical species considered here, but aniline rings rotate around the N—C_{ar} axis and the degree of this rotation is inversely correlated with the predominance of the NH character of the chelate ring (Karabiyik *et al.*, 2009, 2011). The rotation of the aniline ring around the bond joining it to the adjacent aromatic fragment prevents any close parallel stacking and as a result of this rotation, a fragment including the aniline ring in SA derivatives is loosely packed allowing for conformational changes in this part of the molecule. This inference explains why aniline rings occasionally participate in π-stacking interactions involving the hydrogen-bridged chelate ring as the other component.

Distribution of the interplanar distances and β slippage angles, defined as the angle between the normal direction to the chelate ring and the line connecting the centroids of two rings, are shown in Fig. 6. The β values were all less than 30°, while the interplanar distances of pure interactions were accumulated in a somewhat longer region (3.4–3.5 Å) than those of hybrid interactions (3.3–3.4 Å), as shown in Fig. 6(*a*). Owing to the stacking of a large conjugated system comprising the chelate and salicylidene (or aniline) rings, the slippage angles of hybrid interactions are extended in a broader interval than those of pure ones (Fig. 6*b*). Because of the deficiency of σ-orbitals in the chelate ring, hydrogen-bridged ring-assisted π-stacking interactions are not only π-deficient but also σ-deficient interactions. This aspect is of great importance in terms of the fields in which π-interactions play a central role. At the molecular orbital level, the $\pi\cdots\pi$ interactions are subjected to two competitive effects: π–π repulsion and σ–π attraction (Hunter & Sanders, 1990; Hunter, 1993, 1994; Cozzi *et al.*, 1993; Janiak, 2000) as shown in Fig. 7. While the former reduces and perturbs the stability of the interaction by distorting geometry, the latter increases. In hybrid interactions both σ–π attraction and π–π repulsion are more pronounced than in pure $\pi\cdots\pi$ interactions (Fig. 7). Therefore, interplanar distances of pure interactions can reach shorter regions than those of hybrid interactions, as shown in Fig. 6(*a*). Slippage angles, β, for hybrid interactions are higher in value than those of pure interactions, since the σ–π attraction dominates offset π-stacked geometry according to Hunter–Sanders rules (Hunter & Sanders, 1990; Hunter, 1993, 1994; Cozzi *et al.*, 1993; Janiak, 2000). Another reason why the hybrid interactions prefer higher slippage angles than the pure ones (Fig. 6*b*) is to avoid substituent clashing. Steric effects from substituents clashing in hybrid interactions become more evident than those in pure interactions.

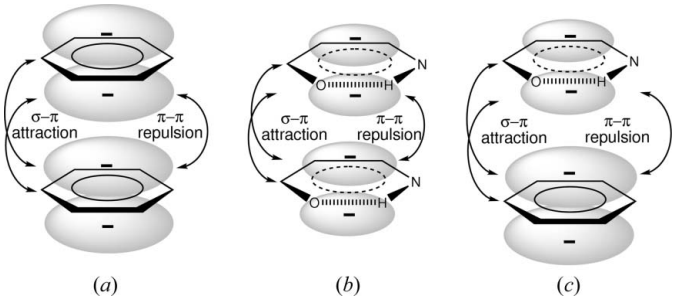

Figure 7
Molecular orbital diagrams of face-to-face conventional $\pi\cdots\pi$ stacking (*a*), pure (*b*) and hybrid (*c*) interactions showing σ–π attraction and π–π repulsion.

The hydrogen-bridged ring-assisted π-stacking interactions of SA derivatives detected in the CSD database were geometrically analyzed according to a phenomenological approach for solid-state packing of conjugated compounds reported by Curtis *et al.* (2004). According to the authors, the extent of distortions from the ideal cofacial π-stacking interactions can be expressed with the aid of pitch-and-roll angles. Pitch-and-roll inclinations for a $\pi\cdots\pi$ stacking interaction are regarded as translation-adjacent molecules relative to one another in the direction of the long and short molecular axis. In addition, the π-stacked interactions are, in general, split into two subclasses: herringbone-type packing with no π-overlap between adjacent molecules prescribed by the condition $P < R$, and lamellar-type packing with a considerable π-overlap between adjacent molecules prescribed by the condition $P > R$. The interrelation between pitch-and-roll angles of the interactions with regard to the total HOMA indices of the interacting ring pairs is illustrated in Fig. 8.

It is inferred from the results in Fig. 8 that all the hydrogen-bridged ring-assisted π-stacking interactions are located in the region of the pitch angle which is greater than the roll angle ($P > R$), indicating substantial spatial π-overlap between adjacent molecules in the solid state. Aromaticity is not an additive quantity due to its locality property. Here the summation of the local aromaticities of the rings participating in the interactions is used to describe the level of π-electron delocalization in the interacting ring pairs, not the aromaticity

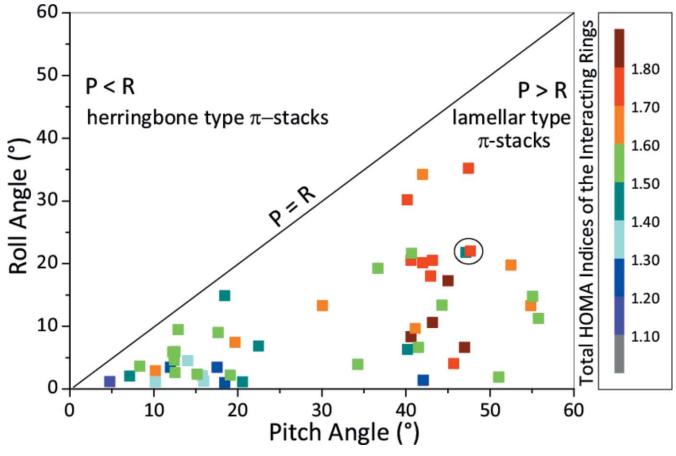

Figure 8
Scattergram for the correlation between pitch (P) and roll (R) angles of the interactions. The cross line depicts the critical situation where $P = R$. Square spots are colored according to the total HOMA indices of the rings involved in hydrogen-bridged ring-assisted π-stacking interactions. The spots relating to the compound are circled.

of the fragments formed by two interacting rings as a whole. Highly aromatic ring pairs participating in such interactions whose total HOMA indices are greater than 1.70 spread out in the region of the large pitch angles, especially $P > 40^\circ$ (Fig. 8). Large pitch angles reducing the substantial spatial overlap between adjacent molecules in the π-stacks have been expectedly observed for higher π-delocalization levels. On the other hand, moderately or weakly aromatic ring pairs are concentrated in the region of small roll ($< 10^\circ$) and relatively small pitch ($< 25^\circ$) angle due to slight π-electron repulsion between interacting ring pairs. Most of the hydrogen-bridged ring-assisted π-stacking interactions have roll angles less than 20°, maintaining substantial spatial overlap between adjacent molecules in the lamellar π-stack. In this respect it should be underscored that the aromaticity of certain molecular fragments in SA derivatives plays an essential role in controlling the molecular aggregation patterns in the solid state by accompanying changes in their molecular building blocks.

5. Conclusions

The present study ends the validity of conventional judgment which states that $\pi\cdots\pi$ stacking interactions are observed between two aromatic rings formed by covalent bonds, or two metallacycles regarded as a kind of chelate ring, by showing that such interactions can also operate in systems containing hydrogen-bridged quasi-aromatic rings. In salicylidene derivatives most of these interactions are observed between the salicylidene and chelate rings. The aromaticity of the chelate ring is increased with the growing predominance of the NH tautomers or equivalently with a decreasing aromaticity of the salicylidene ring, behaving as a π-donor to the chelate ring. What is unusual in these π-stacking interactions is that they involve chelate rings having formally vacant p-type orbitals. They have been divided into two classes, pure and hybrid $\pi\cdots\pi$ interactions, and are distinguished from the usual $\pi\cdots\pi$ interactions by their formation character, both σ- and π-deficient. Moreover, the σ-deficient character of pure interactions is more pronounced than that of hybrid ones.

As seen, resonance-assisted hydrogen bonds (RAHBs) imply augmented aromaticity within their hydrogen-bridged chelate rings, since the formally vacant low-lying p-type orbital on the proton mediates and facilitates π-delocalization in the chelate ring. The hydrogen-bridged chelate ring-assisted π-stacking interactions are not specific to only SA derivatives in the NH tautomeric form; these interactions may be observed in any other chemical species possessing resonance-assisted intra- or intermolecular hydrogen bonds (Sobczyk *et al.*, 2005; Lyssenko & Antipin, 2006; Sanz *et al.*, 2007). More importantly, bearing in mind that RAHBs are observed for nucleic base pairing (Kurczab *et al.*, 2010), hydrogen-bridged ring-assisted π-stacking interactions between adjacent nucleic acid bases which are positioned nearly perpendicular to the length of the DNA strands may be observed in DNA structure. Therefore, it can be stated that such interactions supply new insights in understanding the reasons for stabilization of the consecutive base pairs in the double-helix structure of DNA. Our quantum chemical studies regarding the importance of hydrogen-bridged ring-assisted π-stacking interactions in the fields mentioned above are in progress.

This study was supported under grant F.279 by Ondokuz Mayıs University Research Fund.

References

Allali, M., Jaud, J., Habbadi, N., Dartiguenave, M., Beauchamp, A. L. & Benoist, E. (2009). *Eur. J. Inorg. Chem.* pp. 1488–1494.

Amimoto, K. & Kawato, T. (2005). *J. Photochem. Photobiol. C*, **6**, 207–226.

Banerjee, S., Adarsh, N. N. & Dastidar, P. (2009). *CrystEngComm*, **11**, 746–749.

Bernstein, J., Davis, R. E., Shimoni, L. & Chang, N.-L. (1995). *Angew. Chem. Int. Ed. Engl.* **34**, 1555–1573.

Blanco, V., Abella, D., Pía, E., Platas-Iglesias, C., Peinador, C. & Quintela, J. M. (2009). *Inorg. Chem.* **48**, 4098–4107.

Bogdanovic, G. A., Bire, A. S. & Zaric, S. D. (2002). *Eur. J. Inorg. Chem.* pp. 1599–1602.

Bondi, A. (1964). *J. Phys. Chem.* **68**, 441–451.

Bruno, I. J., Cole, J. C., Edgington, P. R., Kessler, M., Macrae, C. F., McCabe, P., Pearson, J. & Taylor, R. (2002). *Acta Cryst.* B**58**, 389–397.

Bultinck, P., Rafat, M., Ponec, R., Van Gheluwe, B., Carbó-Dorca, R. & Popelier, P. (2006). *J. Phys. Chem. A*, **110**, 7642–7648.

Castiñeiras, A., Sicilia-Zafra, A. G., González-Pérez, J. M., Choque-sillo-Lazarte, D. & Niclós-Gutiérrez, J. (2002). *Inorg. Chem.* **41**, 6956–6958.

Chen, Z., Wannere, C. S., Corminboeuf, C., Puchta, R. & Schleyer, P. R. (2005). *Chem. Rev.* **105**, 3842–3888.

Churchill, C. D. & Wetmore, S. D. (2009). *J. Phys. Chem. B*, **113**, 16046–16058.

Cohen, M. D. & Schmidt, G. M. J. (1962). *J. Chem. Soc.* pp. 2442–2446.

Cohen, M. D., Schmidt, G. M. J. & Flavian, S. (1964). *J. Chem. Soc.* pp. 2041–2051.

Cozzi, F., Cinquini, M., Annuziata, R. & Siegel, J. S. (1993). *J. Am. Chem. Soc.* **115**, 5330–5331.

Craven, E., Zhang, C., Janiak, C., Rheinwald, G. & Lang, H. (2003). *Z. Anorg. Allg. Chem.* **629**, 2282–2290.

Curtis, M. D., Cao, J. & Kampf, J. W. (2004). *J. Am. Chem. Soc.* **126**, 4318–4328.

Cyrański, M. K. (2005). *Chem. Rev.* **105**, 3773–3811.

Cyrañski, M. K., Krygowski, T. M., Katritzky, A. R. & Schleyer, P. R. (2002). *J. Org. Chem.* **67**, 1333–1338.

Cyrański, M. K., Schleyer, P. v. R., Krygowski, T. M., Jiao, H. & Hohlneicher, G. (2003). *Tetrahedron*, **59**, 1657–1665.

Dance, I. (2003). *CrystEngComm*, **5**, 208–221.

Dominiak, P. M., Grech, E., Barr, G., Teat, S., Mallinson, P. & Woźniak, K. (2003). *Chem. Eur. J.* **9**, 963–970.

Dziembowska, T. & Rozwadowski, Z. (2001). *Curr. Org. Chem.* **5**, 289–313.

Egbe, D. A. M., Türk, S., Rathgeber, S., Kuhnlenz, F., Jadhav, R., Wild, A., Birckner, E., Adam, G., Pivrikas, A., Cimrova, V., Knor, G., Sariciftci, N. S. & Hoppe, H. (2010). *Macromolecules*, **43**, 1261–1269.

Fabian, W. M. F., Antonov, L., Nedeltcheva, D., Kamounah, F. S. & Taylor, P. J. (2004). *J. Phys. Chem. A*, **108**, 7603–7612.

Farrugia, L. J. (1997). *J. Appl. Cryst.* **30**, 565.

Farrugia, L. J. (1999). *J. Appl. Cryst.* **32**, 837–838.

Fernandez, J. J., Fernandez, A., Lopez-Torres, M., Vazquez-Garcia, D., Rodriguez, A., Varela, V. & Vila, J. M. (2009). *J. Organomet. Chem.* **694**, 2234–2245.

Filarowski, A. (2005). *J. Phys. Org. Chem.* **18**, 686–698.

Filarowski, A., Kochel, A., Cieslik, K. & Koll, A. (2005). *J. Phys. Org. Chem.* **18**, 986–993.

Filarowski, A., Koll, A. & Glowiak, T. (2002). *J. Mol. Struct.* **615**, 97–108.

Garcia-Baez, E. V., Martinez-Martinez, F. J., Hopfl, H. & Padilla-Martinez, I. I. (2003). *Cryst. Growth Des.* **3**, 35–45.

Grabowski, S. J. (2001). *J. Mol. Struct.* **562**, 137–143.

Grabowski, S. J. (2002). *Monatsh. Chem.* **133**, 1373–1380.

Grabowski, S. J. (2003). *J. Phys. Org. Chem.* **16**, 797–802.

Grabowski, S. J. (2007). *J. Mol. Struct. Theochem*, **811**, 61–67.

Holy, A., Moreno, V., Operschall, B. P. & Sigel, H. (2009). *Inorg. Chim. Acta*, **362**, 799–810.

Hunter, C. A. (1993). *Angew. Chem. Int. Ed. Engl.* **32**, 1584–1586.

Hunter, C. A. (1994). *Chem. Soc. Rev*. **23**, 101–109.

Hunter, C. A., Lawson, K. R., Perkins, J. & Urch, C. J. (2001). *J. Chem. Soc. Perkin Trans. 2*, pp. 651–669.

Hunter, C. A. & Sanders, J. K. M. (1990). *J. Am. Chem. Soc.* **112**, 5525–5534.

Janiak, C. (2000). *J. Chem. Soc. Dalton Trans.* pp. 3885–3896.

Janzen, D. E., Burand, M. W., Ewbank, P. C., Pappenfus, T. M., Higuchi, H., da Silva Filho, D. A., Young, V. G., Brédas, J. L. & Mann, K. R. (2004). *J. Am. Chem. Soc.* **126**, 15295–15308.

Kar, T., Bettinger, H. F., Scheiner, S. & Roy, A. K. (2008). *J. Phys. Chem. C*, **112**, 20070–20075.

Karabiyik, H., Erdem, O., Aygun, M., Guzel, B. & Garcia-Granda, S. (2010). *J. Inorg. Organomet. Polym.* **20**, 142–151.

Karabıyık, H., Güzel, B., Aygün, M., Boğa, G. & Büyükgüngör, O. (2007). *Acta Cryst.* C**63**, o215–o218.

Karabiyik, H., Ocak-Iskeleli, N., Petek, H., Albayrak, C. & Agar, E. (2008). *J. Mol. Struct.* **873**, 130–136.

Karabiyik, H., Petek, H., Iskeleli, N. O. & Albayrak, C. (2009). *Struct. Chem.* **20**, 1055–1065.

Karabiyik, H., Sevincek, R., Petek, H. & Aygun, M. (2011). *J. Mol. Mod.* **17**, 1295–1309.

Krygowski, T. M. (1993). *J. Chem. Inf. Comput. Sci.* **33**, 70–78.

Krygowski, T. M. & Cyrański, M. K. (2001). *Chem. Rev*. **101**, 1385–1419.

Krygowski, T. M. & Cyrański, M. K. (2004). *Phys. Chem. Phys.* **6**, 249–255.

Krygowski, T. M., Wozniak, K., Anulewicz, R., Pawlak, D., Kolodziejski, W., Grech, E. & Szady, A. (1997). *J. Phys. Chem. A*, **101**, 9399–9404.

Kumagai, H., Akita-Tanaka, M., Kawata, S., Inoue, K., Kepert, C. J. & Kurmoo, M. (2009). *Cryst. Growth Des.* **9**, 2734–2741.

Kurczab, R., Mitoraj, M. P., Michalak, A. & Ziegler, T. (2010). *J. Phys. Chem. A*, **114**, 8581–8590.

Lee, E. C., Hong, B. H., Lee, J. Y., Kim, J. C., Kim, D., Kim, Y., Tarakeshwar, P. & Kim, K. S. (2005). *J. Am. Chem. Soc.* **127**, 4530–4537.

Lyssenko, K. A. & Antipin, M. Y. (2006). *Russ. Chem. Bull.* **55**, 1–15.

Marsden, J. A., Miller, J. J., Shirtcliff, L. D. & Haley, M. M. (2005). *J. Am. Chem. Soc.* **127**, 2464–2476.

Masui, H. (2001). *Coord. Chem. Rev.* **219–221**, 957–992.

Medaković, V. B., Milcić, M. K., Bogdanović, G. A. & Zarić, S. D. (2004). *J. Inorg. Biochem.* **98**, 1867–1873.

Mukhopadhyay, U., Choquesillo-Lazarte, D., Niclos-Gutierrez, J. & Bernal, I. (2004). *CrystEngComm*, **6**, 627–632.

Müller, P., Herbst-Irmer, R., Spek, A. L., Schneider, T. R. & Sawaya, M. R. (2006). *Crystal Structure Refinement*, edited by P. Müller, pp. 7–25. Oxford University Press.

Noveron, J. C., Lah, M. S., Del Sesto, R. E., Arif, A. M., Miller, J. S. & Stang, P. J. (2002). *J. Am. Chem. Soc.* **124**, 6613–6625.

Olenik, B., Boese, R. & Sustmann, R. (2003). *Cryst. Growth Des.* **3**, 175–181.

Ośmiałowski, B., Raczyńska, E. D. & Krygowski, T. M. (2006). *J. Org. Chem.* **71**, 3727–3736.

Osuna, S., Poater, J., Bofill, M., Alemany, P. & Sola, M. (2006). *Chem. Phys. Lett.* **428**, 191–195.

Palusiak, M. & Krygowski, T. M. (2007). *Chem. Eur. J.* **13**, 7996–8006.

Petek, H., Albayrak, Ç., Ağar, E. & Kalkan, H. (2006). *Acta Cryst.* E**62**, o3685–o3687.

Petek, H., Albayrak, C., Odabasoglu, M., Senel, I. & Buyukgungor, O. (2008). *J. Chem. Cryst.* **38**, 901–905.

Petek, H., Albayrak, C., Odabasoglu, M., Senel, I. & Buyukgungor, O. (2010). *Struct. Chem.* **21**, 681–690.

Philip, V., Suni, V., Kurup, M. R. P. & Nethaji, M. (2004). *Polyhedron*, **23**, 1225–1233.

Poater, J., Duran, M., Solà, M. & Silvi, B. (2005). *Chem. Rev.* **105**, 3911–3947.

Poater, J., Fradera, X., Duran, M. & Solà, M. (2003). *Chem. Eur. J.* **9**, 400–406.

Reger, D. L., Horger, J., Smith, M. D. & Long, G. J. (2009). *Chem. Commun.* pp. 6219–6221.

Reger, D. L., Sirianni, E., Horger, J. J. & Smith, M. D. (2010). *Cryst. Growth Des.* **10**, 386–393.

Ringer, A. L. & Sherrill, C. D. (2009). *J. Am. Chem. Soc.* **131**, 4574–4575.

Sanz, P., Mó, O., Yañez, M. & Elguero, J. (2007). *J. Phys. Chem. A*, **111**, 3585–3591.

Schaad, L. J. & Hess, B. A. (2001). *Chem. Rev.* **101**, 1465–1476.

Schleyer, P. v. R., Maerker, C., Dransfeld, A., Jiao, H., Hommes, N. J. R. v. E. (1996). *J. Am. Chem. Soc.* **118**, 6317–6318.

Schneider, H.-J. (2009). *Angew. Chem. Int. Ed.* **48**, 3924–3977.

Serrano-Becerra, J. M., Hernandez-Ortega, S., Morales-Morales, D. & Valdes-Martinez, J. (2009). *CrystEngComm*, **11**, 226–228.

Sheldrick, G. M. (2008). *Acta Cryst.* A**64**, 112–122.

Sobczyk, L., Grabowski, S. J. & Krygowski, T. M. (2005). *Chem. Rev.* **105**, 3513–3560.

Spek, A. L. (2009). *Acta Cryst.* D**65**, 148–155.

Sredojevic, D. N., Tomic, Z. D. & Zaric, S. D. (2010). *Cryst. Growth Des.* **10**, 3901–3908.

Steiner, T. (1998). *J. Phys. Chem. A*, **102**, 7041–7052.

Stoe & Cie (2002*a*). *X-AREA*, Version 1.18. Stoe & Cie, Darmstadt.

Stoe & Cie (2002*b*). *X-RED32*, Version 1.04. Stoe & Cie, Darmstadt.

Tomic, Z. D., Leovac, V. M., Jacimovic, Z. K., Giester, G. & Zaric, S. D. (2006). *Inorg. Chem. Commun.* **9**, 833–835.

Tomic, Z. D., Leovac, V. M., Pokorni, S. V., Zobel, D. & Zaric, S. D. (2003). *Eur. J. Inorg. Chem.* pp. 1222–1226.

Tomic, Z. D., Novakovic, S. B. & Zaric, S. D. (2004). *Eur. J. Inorg. Chem.* pp. 2215–2218.

Tsubaki, H., Tohyama, S., Koike, K., Saitoh, H. & Ishitani, O. (2005). *Dalton Trans.* pp. 385–395.

Tsuzuki, S. (2005). *Struct. Bond.* **115**, 149–193.

Wu, J.-Y., Hsu, H.-Y., Chan, C.-C., Wen, Y.-S., Tsai, C. & Lu, K.-L. (2009). *Cryst. Growth Des.* **9**, 258–262.

Yang, S. Y., Naumov, P. & Fukuzumi, S. (2009). *J. Am. Chem. Soc.* **131**, 7247–7249.

Zheng, Y.-Z., Speldrich, M., Kogerler, P. & Chen, X.-M. (2010). *CrystEngComm*, **12**, 1057–1059.